END
DATE
FILMED

DTIC

1.0

1.1

1.25

45
50
56

2.8
3.2
3.6
40

1.4

2.5
2.2
2.0

1.8

1.6

MICROCOPY RESOLUTION TEST CHART
NATIONAL BUREAU OF STANDARDS-1963-A

LEVEL C

NASA
Technical Paper 1721

AVRADCOM
Technical Report 80-A-2

Calculation of Three-Dimensional Unsteady Transonic Flows Past Helicopter Blades

J. J. Chattot
Aeromechanics Laboratory
AVRADCOM Research and Technology Laboratories
Ames Research Center
Moffett Field, California

NASA

NASA, USAAVRADCOM

TP-1721, TR-80-A-2

Calculation of Three-Dimensional Unsteady Transonic Flows Past Helicopter Blades.

Oct 80

J. J. Chattot

NA.A-A-1891

OCTOBER 1980

DTIC
ELECTE
NOV 3 1980
C

DISTRIBUTION STATEMENT A
Approved for public release;
Distribution Unlimited

388090

CALCULATION OF THREE-DIMENSIONAL UNSTEADY TRANSONIC FLOWS

PAST HELICOPTER BLADES

J. J. Chattot*

Ames Research Center
and
Aeromechanics Laboratory
AVRADCOM Research and Technology Laboratories

SUMMARY

A finite difference code for predicting the high-speed flow over the advancing helicopter rotor is presented. The code solves the low-frequency, transonic small disturbance equation and is suitable for modeling the effects of advancing blade unsteadiness on blades of nearly arbitrary planform. The method employs a quasi-conservative mixed differencing scheme and solves the resulting difference equations by an alternating direction scheme. Computed results show good agreement with experimental blade pressure data and illustrate some of the effects of varying the rotor planform. The flow unsteadiness is shown to be an indispensible part of a transonic solution. It is also shown that, close to the tip at high advance ratio, cross-flow effects can significantly affect the solution.

INTRODUCTION

Air flow past a helicopter rotor blade exhibits many very complex features such as three-dimensional unsteady effects, shock-wave motions, vortex interactions, and stall. A complete numerical simulation cannot even be attempted yet, but it is possible with the present-day computers and numerical methods to model some of these features and acquire a better understanding of some of the mechanisms involved.

The model used in this study is a perfect fluid model that is further simplified by the small-disturbance approximation. Weak, almost normal shock waves are accounted for by retaining the leading nonlinear term in the streamwise direction. This model is useful for simulating the subsonic and transonic flow past the advancing blade. Under these conditions the incidence is usually small, and the results presented correspond to nonlifting blades. A proper wake representation is required to extend this simulation to lifting configurations. Prediction of the complicated rotor vortex structure is not within the scope of the present work.

---

*ONERA exchange scientist.

It is hoped that this report and the code named and referred to hereafter as THREED will be useful tools in their limited scope and that enough flexibility has been built into THREED to allow for later improvement.

This work was done while the author was on assignment at the U.S. Army Aeromechanics Laboratory, Ames Research Center, Moffett Field, California, according to the Memorandum of Understanding (MOU) agreement between Office National D'Etudes et de Recherches Aérospatiales (ONERA), France and U.S. Army at Ames on helicopter research.

The author wishes to express his thanks to Dr. C. Capelier, Director of the Aerodynamics at ONERA and Dr. I. C. Statler, Director of the U.S. Army Aeromechanics Laboratory as well as his colleagues at the Ames Research Center who made this visit possible, and most pleasant. Special thanks go also to Mrs. C. Coulombeix and Mr. Lê of ONERA for the hardship of losing their group leader for nine months. Finally, a "grand merci" to Chris Dolnack for the very good typing.

EQUATION AND BOUNDARY CONDITIONS

The mathematical model used in this report is the three-dimensional unsteady (low-frequency) small-disturbance transonic equation as derived by M. P. Isom (ref. 1, p. 20). This equation is derived in a blade-attached Cartesian coordinate system under the usual assumptions:

$$1 - M^2(1 + \mu)^2 = 0(\delta^{2/3})$$

$$\varepsilon = 0(\delta)$$

where

$M = \dfrac{\Omega R}{a_\infty}$ tip Mach number due to the blade rotation

$\mu = \dfrac{V}{\Omega R}$ advance ratio

δ blade thickness

$\varepsilon = \left(\dfrac{c}{R}\right)^{-1}$ inverse of the aspect ratio

R blade radius

c chord of reference

Ω rotational velocity

a_∞ sound speed

V forward velocity of the rotor

2

In condensed notation the equation can be written:

$$A \frac{\partial^2 \phi}{\partial t \, \partial x} = \frac{\partial}{\partial x} \left[B \frac{\partial \phi}{\partial x} + B' \left(\frac{\partial \phi}{\partial x} \right)^2 \right] + C \frac{\partial^2 \phi}{\partial x \, \partial y} + D \frac{\partial^2 \phi}{\partial y^2} + E \frac{\partial^2 \phi}{\partial z^2} \tag{1}$$

where

$$A = 2M^2 \frac{\epsilon}{\delta^{2/3}} (y + \mu \cos t)$$

$$B = \frac{1 - M^2 (y + \mu \cos t)^2}{\delta^{2/3}}$$

$$B' = \frac{\gamma + 1}{2} M^2 (y + \mu \cos t)$$

$$C = 2M^2 \frac{\epsilon}{\delta^{2/3}} \mu \sin t (y + \mu \cos t)$$

$$D = \frac{\epsilon^2}{\delta^{2/3}}$$

$$E = 1$$

t, x, y, and z are the dimensionless dependent variables normalized by Ω, c, R, and $\delta^{-1/3}$ c, respectively, and γ is the ratio of the specific heats. At each time step NS in THREED, the coefficients are computed and stored in one-dimensional arrays

$$A(J), \ B(J), \ BP(J), \ C(J), \ D(J), \ E(J), \ J = 1, \ \ldots \ JM$$

for all values of the spanwise index J. Allowance is made in the code for a term $A' \partial \phi / \partial t$ for which the value of the coefficient is stored in AP(J) and has been set to zero for all present uses.

Initial and boundary conditions are required. To integrate this equation the initial condition used is usually the quasi-steady solution (i.e., $\phi_{xt} = 0$ in eq. (1)).

On the mean surface of the blade the flow tangency condition is expressed (cf. ref. 1) as:

$$\frac{\partial \phi}{\partial z} = (y + \mu \cos t) f'(x) \quad \text{at} \quad z = 0$$

At the innermost grid location, y_{min}, two boundary conditions can be used:

1. A symmetry condition (equivalent to a flat tunnel wall in wing calculations)

$$\frac{\partial \phi}{\partial y} = 0 \quad \text{(specified by setting JSYM = 1 in THREED)}$$

3

2. A strip-theory condition (used for rotor blades or semi-infinite wings)

$$\frac{\partial^2 \phi}{\partial y^2} = 0$$

In the far field a Dirichlet ($\phi = 0$) or a Newman ($\partial\phi/\partial n = 0$) condition has been used. The upstream boundary is usually taken as the uniform undisturbed flow ($\phi = 0$).

COORDINATE TRANSFORMATION AND THE CORRESPONDING MESH SYSTEM

In order to treat a large class of planform shapes, a coordinate transformation is made prior to the discretization of the equation. This transformation incorporates some one-dimensional stretching capabilities concentrating the mesh in regions of large gradients; in particular, near the surface of the blade, near the leading edge, and near the tip. The coordinate transformation is of the form, $(x,y,z) \rightarrow (\xi,\eta,\zeta)$,

where

$$\xi = \xi(x,y)$$

$$\eta = \eta(y)$$

$$\zeta = \zeta(z)$$

Equation (1) now becomes:

$$A \frac{\partial \xi}{\partial x} \frac{\partial^2 \phi}{\partial t \partial \xi} = B \left(\frac{\partial \xi}{\partial x}\right)^2 \frac{\partial^2 \phi}{\partial \xi^2} + B' \left(\frac{\partial \xi}{\partial x}\right)^3 \frac{\partial}{\partial \xi} \left(\frac{\partial \phi}{\partial \xi}\right)^2 + \left[C \frac{\partial \xi}{\partial x} \frac{\partial \xi}{\partial y} + D \left(\frac{\partial \xi}{\partial y}\right)^2 \right] \frac{\partial^2 \phi}{\partial \xi^2}$$

$$+ \left(C \frac{\partial \xi}{\partial x} \frac{\partial \eta}{\partial y} + 2D \frac{\partial \xi}{\partial y} \frac{\partial \eta}{\partial y} \right) \frac{\partial^2 \phi}{\partial \xi \partial \eta} + D \left(\frac{\partial \eta}{\partial y}\right)^2 \frac{\partial^2 \phi}{\partial \eta^2} + E \left(\frac{\partial \zeta}{\partial z}\right)^2 \frac{\partial^2 \phi}{\partial \zeta^2} + B \frac{\partial^2 \xi}{\partial x^2} \frac{\partial \phi}{\partial \xi}$$

$$+ 2B' \frac{\partial \xi}{\partial x} \frac{\partial^2 \xi}{\partial x^2} \left(\frac{\partial \phi}{\partial \xi}\right)^2 + \left(C \frac{\partial^2 \xi}{\partial x \partial y} + D \frac{\partial^2 \xi}{\partial y^2} \right) \frac{\partial \phi}{\partial \xi} + D \frac{\partial^2 \eta}{\partial y^2} \frac{\partial \phi}{\partial \eta} + E \frac{\partial^2 \zeta}{\partial z^2} \frac{\partial \phi}{\partial \zeta}$$

$$(2)$$

The coefficients in equation (2) are the partial derivatives of the transformation. This form of the equation is called semiconservative; the metric coefficients are brought outside the $\partial/\partial\xi$, $\partial/\partial\eta$, $\partial/\partial\zeta$ symbols. It can be shown that, if the transformation is sufficiently regular, the jump conditions are preserved across a discontinuity.

Computation is made of four first partial derivatives and five second partial derivatives. They are $\partial\xi/\partial x$, $\partial\xi/\partial y$, $\partial\eta/\partial y$, and $\partial\zeta/\partial z$ (called in THREED XIX, XIY, YIY, and ZIZ, respectively) and $\partial^2\xi/\partial x^2$, $\partial^2\xi/\partial x\partial y$, $\partial^2\xi/\partial y^2$, $\partial^2\eta/\partial y^2$, and $\partial^2\zeta/\partial z^2$ (called in THREED XIX2, XIXY, XIY2, YIY2, and ZIZ2,

4

respectively). These quantities are computed at each interior mesh point by using finite difference approximations of the coefficients of the inverse transformation and the following identities:

$$1 = \frac{\partial x}{\partial \xi}\frac{\partial \xi}{\partial x}$$

$$1 = \frac{\partial y}{\partial \eta}\frac{\partial \eta}{\partial y}$$

$$1 = \frac{\partial z}{\partial \zeta}\frac{\partial \zeta}{\partial z}$$

$$0 = \frac{\partial x}{\partial \xi}\frac{\partial \xi}{\partial y} + \frac{\partial x}{\partial \eta}\frac{\partial \eta}{\partial y}$$

and, similarly,

$$0 = \frac{\partial x}{\partial \xi}\frac{\partial^2 \xi}{\partial x^2} + \frac{\partial^2 x}{\partial \xi^2}\left(\frac{\partial \xi}{\partial x}\right)^2$$

$$0 = \frac{\partial x}{\partial \xi}\frac{\partial^2 \xi}{\partial x\,\partial y} + \frac{\partial^2 x}{\partial \xi^2}\frac{\partial \xi}{\partial x}\frac{\partial \xi}{\partial y} + \frac{\partial^2 x}{\partial \xi\,\partial \eta}\frac{\partial \xi}{\partial x}\frac{\partial \eta}{\partial y}$$

$$0 = \frac{\partial y}{\partial \eta}\frac{\partial^2 \eta}{\partial y^2} + \frac{\partial^2 y}{\partial \eta^2}\left(\frac{\partial \eta}{\partial y}\right)^2$$

$$0 = \frac{\partial x}{\partial \xi}\frac{\partial^2 \xi}{\partial y^2} + \frac{\partial x}{\partial \eta}\frac{\partial^2 \eta}{\partial y^2} + \frac{\partial^2 x}{\partial \xi^2}\left(\frac{\partial \xi}{\partial y}\right)^2 + 2\,\frac{\partial^2 x}{\partial \xi\,\partial \eta}\frac{\partial \xi}{\partial y}\frac{\partial \eta}{\partial y} + \frac{\partial^2 x}{\partial \eta^2}\left(\frac{\partial \eta}{\partial y}\right)^2$$

$$0 = \frac{\partial z}{\partial \zeta}\frac{\partial^2 \zeta}{\partial z^2} + \frac{\partial^2 z}{\partial \zeta^2}\left(\frac{\partial \zeta}{\partial z}\right)^2$$

The derivatives $\partial x/\partial \xi$, . . . are evaluated by finite differences at point i,j as

$$\left(\frac{\partial x}{\partial \xi}\right)_{i,j} = \frac{x_{i+1,j} - x_{i-1,j}}{2\Delta\xi}$$

These expressions include second-order terms $[0(\Delta\xi + \Delta\eta)^2 + 0(\Delta\zeta)^2]$. The mesh is constructed in three steps. In the first step the locations of the span-wise stations are defined. The following stations are specified:

y_{min} innermost station on the blade, typically $y_{min} \doteq 0.5$ (y_{min} is referred to as YN in THREED)

y_c a special station on the blade (e.g., a kink in the planform), typically $y_c \doteq 0.9$ ($y_c \rightarrow$ YC in THREED)

y_d the tip of the blade $y_d = 1$ ($y_d \rightarrow$ YD in THREED)

y_{max} outermost radial station, typically $y_{max} \simeq 1.5$ ($y_x \rightarrow$ YX in THREED)

In addition to these real numbers the corresponding integers (JC $\leq$ JD) must be defined. This determines how many stations for computation are located between 1 (y_{min}) and JC (y_c), JC (y_c) and JD (y_d), and JD (y_d) and JM (y_{max}). The following analytical expressions are used to define the mesh stations:

$$J > JD \qquad Y(J) = YX + \cos\left(\frac{\pi}{2}\frac{\eta - \eta_D}{1 - \eta_D}\right)(YD - YX)$$

$$J \leq JC \qquad Y(J) = YN + \cos\left(\frac{\pi}{2}\frac{\eta - \eta_c}{\eta_c}\right)(YC - YN)$$

$$JC < J \leq JD \qquad Y(J) = YC + \frac{\eta - \eta_c}{\eta_D - \eta_c}(YD - YC)$$

where the variable η is defined between 0 and 1 by

$$\eta = \frac{J - 1}{JM - 1}$$

The planform of the blade then yields the locations x_a and x_f of the leading and trailing edges as functions of J. For this purpose, a piecewise analytical representation is made of the planform. The chordwise coordinate transformation has no radial dependence for all points beyond the tip. In THREED x_a and x_f are called XA(J) and XF(J).

The second step in mesh construction, in the chordwise direction, is defining

x_{min} upstream boundary, typically $x_{min} \simeq -8$ ($x_{min} \rightarrow$ XN)

x_{max} downstream boundary, typically $x_{max} \simeq 6$ ($x_{max} \rightarrow$ XX)

and the indices IA $\leq$ IF which determine how many stations are located between 1 (x_{min}) and IA (x_a), IA (x_a) and IF (x_f), and IF (x_f) and IM (x_{max}). Similar analytical expressions are used to define the mesh stations in x:

$$I > IF \qquad X(I,J) = XX + \cos\left(\frac{\pi}{2}\frac{\xi - \xi_F}{1 - \xi_F}\right)[XF(J) - XX]$$

$$I \leq IA \qquad X(I,J) = XN + \cos\left(\frac{\pi}{2}\frac{\xi - \xi_A}{-1 - \xi_A}\right)[XA(J) - XN]$$

$$IA < I \leq IF \qquad X(I,J) = XA(J) + \left[1 - \cos\left(\frac{\pi}{2}\frac{\xi - \xi_A}{\xi_F - \xi_A}\right)\right][XF(J) - XA(J)]$$

6

where the variable ξ is defined between -1 and 1 by

$$\xi = -1 + \frac{2(I - 1)}{IM - 1}$$

In the third step in the vertical direction the following are defined:

z_{min} lower boundary, typically $z_{min} \doteq -3$ ($z_{min} \rightarrow ZN$)

z_{max} upper boundary, typically $z_{max} \doteq 3$ ($z_{max} \rightarrow ZX$)

and the indices $KU = KO + 1$ which determine how many stations are located between 1 (z_{min}) and KO (nearest to the lower surface of the blade), and KU (nearest to the upper surface of the blade) and KM (z_{max}). The mesh stations in z are defined by using the analytical expressions:

$$K > KO \qquad Z(K) = ZX - \cos\left(\frac{\pi}{2}\zeta\right)ZX$$

$$K \leq KO \qquad Z(K) = ZN - \cos\left(\frac{\pi}{2}\zeta\right)ZN$$

where ζ is defined between -1 and 1 by

$$\zeta = -1 + \frac{2(k - 1)}{KM - 1}$$

The mesh dimensions in the code are set up to allow for maximums of $IM = 64$, $JM = 32$, and $KM = 32$.

FINITE DIFFERENCE SCHEME

In equation (1), the nonlinear term $(\partial/\partial x)[B(\partial\phi/\partial x) + B'(\partial\phi/\partial x)^2]$, which is often written nonconservatively as $V\phi_{xx}$, is responsible for the mixed character of the flow. It is well established that a mixed scheme must be used for the nonlinear flux discretization (refs. 2 and 3), given as follows for a uniform mesh spacing:

Let $\qquad V_i = B + 2B' \dfrac{\phi_{i+1} - \phi_{i-1}}{2\Delta x}$

In the following four cases to be considered the nonlinear term is discretized; e.g.,

Case 1 $V_i \geq 0$ $V_{i-1} \geq 0$ (subsonic point)

Discretization: $\quad V_i \dfrac{\phi_{i+1} - 2\phi_i + \phi_{i-1}}{\Delta x^2}$

(the indices j and k, which are invariant, are not indicated).

7

Case 2 $V_i < 0$ $V_{i-1} < 0$ (Supersonic point)

Discretization: $V_{i-1} \dfrac{\phi_i - 2\phi_{i-1} + \phi_{i-2}}{\Delta x^2}$

Case 3 $V_i < 0$ $V_{i-1} \geq 0$ (sonic point)

Discretization: $V_i \dfrac{\phi_i - 2\phi_{i-1} + \phi_{i-2}}{\Delta x^2}$

Case 4 $V_i \geq 0$ $V_{i-1} < 0$ (shock point)

Discretization: $V_i \dfrac{\phi_{i+1} - 2\phi_i + \phi_{i-1}}{\Delta x^2} + V_{i-1} \dfrac{\phi_i - 2\phi_{i-1} + \phi_{i-2}}{\Delta x^2}$

In contrast to most small disturbance codes (typified by refs. 4 and 5), the discretization of the sonic point (case 3) eliminates some spurious oscillations that appear when the sonic line is located close to the leading edge of a blunt airfoil in a region where the flow experiences a rapid acceleration. It can be shown that the discretization that is proposed here is consistent with the equation, but it is not strictly conservative. However, the error of conservation is small, and not larger than $O(\Delta x)$. The shock-point discretization, however, ensures conservation of mass at the shock point.

The next term in equation (1) is the cross-derivative term. This term is small inboard where the flow is subsonic and two-dimensional. However, for large advance ratios ($\mu \doteq 0.5$) and for values of azimuth and radius where the transonic flow has a large radial component, its effects cannot be neglected. In fact, in these cases the cross-derivative term, which is usually treated explicitly (i.e., always at the previous time level (ref. 5)), has a destabilizing effect and can strongly reduce the time step required for maintaining overall stability.

For values of $C \geq 0$, corresponding to a negative sweep angle, the cross-derivative term is discretized as:

$$c_j \frac{\phi_{i,j+1} - \phi_{i,j} - \phi_{i-1,j+1} + \phi_{i-1,j}}{\Delta x \, \Delta y}$$

For values of $C < 0$, corresponding to a positive sweep angle, the following discretization is used:

$$c_j \frac{\phi_{i,j} - \phi_{i,j-1} - \phi_{i-1,j} + \phi_{i-1,j-1}}{\Delta x \, \Delta y}$$

The schemes that are presented for uniform mesh spacing extend readily to the mesh obtained from the coordinate transformation. The coefficient of the cross-derivative is now

8

$$c \frac{\partial \xi}{\partial x} \frac{\partial \eta}{\partial y} + 2D \frac{\partial \xi}{\partial y} \frac{\partial \eta}{\partial y}$$

For discretization of the term $c(\partial\xi/\partial x)(\partial\xi/\partial y)(\partial^2\phi/\partial\xi^2)$ a centered scheme is used at all points:

$$c_j \frac{\partial \xi_{i,j}}{\partial x} \frac{\partial \xi_{i,j}}{\partial y} \frac{\phi_{i+1} - 2\phi_i + \phi_{i-1}}{\Delta \xi^2}$$

SOLUTION ALGORITHM

The time-accurate integration is obtained by using an Alternate Direction Implicit (ADI) scheme that breaks the three-dimensional problem into three one-dimensional problems in each coordinate direction. The advantage of this scheme is its inherent stability, at least in the case of a linear equation, regardless of the local Courant number. Indeed, when solving a complicated problem, in a mesh where the cell sizes may vary by one or more orders of magnitudes, it would be very time-consuming to limit the time step to satisfy the Courant number associated with the smallest cell.

However, since the equation being solved is nonlinear, there is a practical limitation which can be associated with vortex shedding in lifting cases or configurations with shock motion. This means that the cell sizes must never be so small on the airfoil surface and near the trailing edge that the allowable time step for maintaining stability is unnecessarily limited.

A Crank-Nicholson averaging between the levels n and $n + 1$ is used since it can be shown on the linearized equation that a stable scheme results.

The three steps of the ADI-Crank-Nicholson algorithm are as follows:

Step 1

$$A \frac{\partial \xi}{\partial x} \frac{\partial}{\partial \xi} \left(\frac{\tilde{\phi} - \phi^n}{\Delta t} \right) = \frac{B}{2} \left(\frac{\partial \xi}{\partial x} \right)^2 \left(\frac{\partial^2 \phi^n}{\partial \xi^2} + \frac{\partial^2 \tilde{\phi}}{\partial \xi^2} \right) + B' \left(\frac{\partial \xi}{\partial x} \right)^3 \frac{\partial}{\partial \xi} \frac{\partial \phi^n}{\partial \xi} \frac{\partial \tilde{\phi}}{\partial \xi} + \frac{D}{2} \left(\frac{\partial \xi}{\partial y} \right)^2 \left(\frac{\partial^2 \phi^n}{\partial \xi^2} + \frac{\partial^2 \tilde{\phi}}{\partial \xi^2} \right)$$

$$+ \left(c \frac{\partial \xi}{\partial x} \frac{\partial \eta}{\partial y} + 2D \frac{\partial \xi}{\partial y} \frac{\partial \eta}{\partial y} \right) \frac{\partial^2 \phi^n}{\partial \xi \partial \eta} \qquad + c \frac{\partial \xi}{\partial x} \frac{\partial \xi}{\partial y} \frac{\partial^2 \phi^n}{\partial \xi^2}$$

$$+ D \left(\frac{\partial \eta}{\partial y} \right)^2 \frac{\partial^2 \phi^n}{\partial \eta^2} + E \left(\frac{\partial \zeta}{\partial z} \right)^2 \frac{\partial^2 \phi^n}{\partial \zeta^2}$$

$$+ \frac{B}{2} \frac{\partial^2 \xi}{\partial x^2} \left(\frac{\partial \phi^n}{\partial \xi} + \frac{\partial \tilde{\phi}}{\partial \xi} \right) + 2B' \frac{\partial \xi}{\partial x} \frac{\partial^2 \xi}{\partial x^2} \frac{\partial \phi^n}{\partial \xi} \frac{\partial \tilde{\phi}}{\partial \xi} + \frac{D}{2} \frac{\partial^2 \xi}{\partial y^2} \left(\frac{\partial \phi^n}{\partial \xi} + \frac{\partial \tilde{\phi}}{\partial \xi} \right)$$

$$+ D \frac{\partial^2 \eta}{\partial y^2} \frac{\partial \phi^n}{\partial \eta} + E \frac{\partial^2 \zeta}{\partial z^2} \frac{\partial \phi^n}{\partial \zeta} \qquad + c \frac{\partial^2 \xi}{\partial x \partial y} \frac{\partial \phi^n}{\partial \xi}$$

It should be noted that the underlined terms are treated explicitly. However, an implicit scheme can easily be devised based on switching from a centered difference approximation to $\partial^2\phi/\partial\xi^2$ when $(c\partial\xi/\partial x)(\partial\xi/\partial y) \geq 0$, and to an upwind difference approximation when $(c\partial\xi/\partial x)(\partial\xi/\partial y) < 0$. Test results for a swept tip showed very little difference between the implicit treatment and the explicit scheme given previously.

Step 2

$$A\frac{\partial\xi}{\partial x}\frac{\partial}{\partial\xi}\left(\frac{\tilde{\tilde{\phi}} - \tilde{\phi}}{\Delta t}\right) = \frac{1}{2}\left(c\frac{\partial\xi}{\partial x}\frac{\partial\eta}{\partial y} + 2D\frac{\partial\xi}{\partial y}\frac{\partial\eta}{\partial y}\right)\left(\frac{\partial^2\tilde{\tilde{\phi}}}{\partial\xi\partial\eta} - \frac{\partial^2\phi^n}{\partial\xi\partial\eta}\right)$$

$$+ \frac{D}{2}\left(\frac{\partial\eta}{\partial y}\right)^2\left(\frac{\partial^2\tilde{\tilde{\phi}}}{\partial\eta^2} - \frac{\partial^2\phi^n}{\partial\eta^2}\right) + \frac{D}{2}\frac{\partial^2\eta}{\partial y^2}\left(\frac{\partial\tilde{\tilde{\phi}}}{\partial\eta} - \frac{\partial\phi^n}{\partial\eta}\right)$$

Step 3

$$A\frac{\partial\xi}{\partial x}\frac{\partial}{\partial\xi}\left(\frac{\phi^{n+1} - \tilde{\tilde{\phi}}}{\Delta t}\right) = \frac{E}{2}\left(\frac{\partial\zeta}{\partial z}\right)^2\left(\frac{\partial^2\phi^{n+1}}{\partial\zeta^2} - \frac{\partial^2\phi^n}{\partial\zeta^2}\right) + \frac{E}{2}\frac{\partial^2\zeta}{\partial z^2}\left(\frac{\partial\phi^{n+1}}{\partial\zeta} - \frac{\partial\phi^n}{\partial\zeta}\right)$$

After these equations are discretized according to the method discussed in the Finite Difference Scheme section, the algebraic system is inverted by using a tridiagonal or quadradiagonal direct solver. Particular attention is given, when defining the finite difference analogues, to ensure that the main diagonal term could be chosen as pivot in the elimination process. All the terms, which are treated implicitly, contribute to the main diagonal with the same sign.

Each complete time step requires approximately 2.5 sec of CPU time of the CDC 7600 computer. A rectangular blade computation requires approximately half an hour of total run time. For swept tips, where there is a more severe time-step limitation, the total run time is an hour. The corresponding mesh is composed of approximately 35,000 nodes.

RESULTS

Some three-dimensional steady (hover) flows are simulated for three blade geometries: a rectangular blade, a swept-tip blade, and a blade combining a swept and parabolic tip (fig. 1). The pressure distributions are presented for three sections of the blades in figures 2(a-c) for blade A, figures 2(d-f) for blade B, and figures 2(g-i) for blade C. As can be seen, the effect of sweep is favorable inboard. The shock waves either are weakened or disappear on blade C. Close to the tip, however, the opposite trend seems to occur, with blade C experiencing the largest supersonic pocket. The global effect is favorable for the swept tips in hover.

Three-dimensional unsteady flows past a rectangular blade of aspect ratio $R = 7$, have been computed at Mach numbers $M = 0.6$ and advance ratios (μ) of 0.45, 0.5, and 0.55. The blade has no twist and is equipped with a symmetric NACA 00XX profile of varying thickness along the span. ONERA experimental

10

data for the same rotors and test conditions are available for comparison (ref. 4). Figure 3 shows the radial stations for the experimental pressure measurements. The corresponding results are shown in figures 4(a-c) for the azimuth of 60° and in figures 4(d-f) for the azimuth of 120° at the lowest advance ratio. For the advance ratio of $\mu = 0.5$, the results are presented in figures 4(g-l). Figures 4(m-r) show results for $\mu = 0.55$ for the same two azimuth angles of 60° and 120°. Also plotted in these figures are the quasi-steady results, which correspond to $\partial^2 \phi / \partial t \partial x = 0$. As can be seen, the unsteady results agree better with the experimental results, indicating a non-negligible unsteady term $\partial^2 \phi / \partial t \partial x$. Furthermore, a comparison of the quasi-steady solutions at azimuth angles of 60° and 120° exhibits the influence of the cross-derivative $\partial^2 \phi / \partial x \partial y$, which increases toward the tip.

THREED CODE

THREED has been coded in FORTRAN by using only standard statements. In its present form it is adapted to the CDC 7600 computer of the Ames Research Center, NASA, Moffett Field, California. The Small Core Memory (SCM) length is 27,257 decimal words and the Large Core Memory (LCM) length is 131,072 decimal words. THREED is divided into one main program and four subroutines:

SUBROUTINE MESH	defines the mesh and computes the metric coefficients
SUBROUTINE SLOPE	computes the slope of the blade at each point
SUBROUTINE POT	integrates the potential equation
SUBROUTINE CP	computes the pressure coefficient on the blade

The data as they are read in and printed out are shown in appendix A. The values shown correspond to the results plotted in figure 4(g-l). A short explanation of the parameters as well as the notation in THREED follows:

i)   HM = 0.6   Mach number
      ALPHO = 0   mean incidence of the sinusoidal motion, deg
      DALPH = 0   amplitude of the incidence variation, deg
       IROT = 1   rotating blade case
       IROT = 0   fixed blade or wing case
         AV = 0.5   advance ratio
         GM = 1.4   ratio of specific heats

ii)   NSTP = 601   number of time steps
       ITER = 400   number of iteration steps
        DTN = 0.0001 minimum time-step size in the relaxation process (rad)
        DTX = 0.01   maximum time-step size in the relaxation process (rad)
       NMOD = 8   number of elements in the time-step sequence based on
                     DTN and DTX
         TI = -1.5708 initial time (rad)
        NPR = 100   time step at which results are printed

iii)   YC = 0.9   location of the kink or a special span location
        YD = 1   tip of the blade

KSG = 1	indicates that the blade is symmetric with respect to z = 0	
KSG = 0	indicates that the blade is not symmetric	
DEL = 0.12	thickness of the basic profile as defined subsequently	
AR = 7	aspect ratio of the blade	

iv)
JYSM = 0	indicates that a strip-theory condition is used at the root
JYSM = 1	indicates that a symmetry condition is used at the root
KSYM = 1	there is a lower-upper symmetry
KSYM = 0	there is no lower-upper symmetry
KGRAD = 1	a Neuman boundary condition is used
KGRAD = 0	a Dirichlet boundary condition is used

v)
IM = 64	number of mesh points in the ξ direction (≤ 64)
JM = 32	number of mesh points in the η direction (≤ 32)
KM = 32	number of mesh points in the ζ direction (≤ 32)

vi)
IA = 18	leading-edge index (IA $\leq$ IF)
IF = 48	trailing-edge index (IF $\leq$ 64)
JC = 11	kink station index (JC $\leq$ JD)
JD = 21	tip station (JD $\leq$ 32)
KO = 16	lower-surface index
KU = 17	upper-surface index (KU = KO + 1 $\leq$ 32)

vii)
XN = -8	location of most upstream surface
XX = 6	location of most downstream surface
YN = 0.5	location of innermost surface
YX = 1.5849	location of outermost surface
ZN = -3	location of most bottom surface
ZX = 3	location of most tip surface

viii) The basic airfoil is defined by two sets of values representing the abscissas and the ordinates of points on the profile. The maximum number of points is 101. The points are distributed in sequential order around the air-foil, starting from the trailing edge describing the upper surface, then the lower surface, and then back to the trailing edge.

NP = 101	total number of points (≤ 101)
(NP + 1)/2	must correspond to the leading edge

When the geometry changes rapidly it is preferable to concentrate the points near the leading and trailing edges in order to ensure the best pos-sible accuracy for linear interpolation. The coordinate profile at the mesh location N is

XP (N)	abscissa	of point N
ZP (N)	ordinate	

The planform geometry of the blade is defined by piecewise-analytic formulas in the subroutine MESH. An example is given in appendix B for a swept tip. The functions XA(J) and XF(J) are defined in the loop starting with

12

```
77            DO 6 J = 1, JM
```

and ending with

```
87            6 CONTINUE
```

as shown in the box.

CONCLUSIONS

A finite difference code for predicting the high-speed flow over an advancing helicopter rotor is presented. The code solves the low-frequency transonic small disturbance equation and is suitable for modeling the effects of three-dimensional advancing blade unsteadiness. This work was inspired by a similar method developed by F. X. Caradonna (ref. 5). However, the computer code THREED incorporates some important new features, especially the capability for treating nonrectangular blade tips. Computed results show good agreement with experimental blade pressure data and illustrate some of the effects of varying the rotor planform. The flow unsteadiness is shown to be an indispensible part of a transonic solution. It is also shown that close to the tip at high advance ratio, cross-flow effects can significantly affect the solution.

Ames Research Center
    National Aeronautics and Space Administration
        and
Aeromechanics Laboratory
    AVRADCOM Research and Technology Laboratories
        Moffett Field, Calif. 94035, April 10, 1980

13

APPENDIX A

SAMPLE OF DATA AS READ IN AND PRINTED OUT OF CDC 7600 COMPUTER

MACH NUMBER	MEAN INCIDENCE	INCIDENCE VARIATION	ROTATION Y/N	ADVANCE RATIO	HEAT RATIO
.6	0.	0.	1	.5	1.4

NO.TIME STEPS	NO.STEPS RELAXATION	MIN STEP RELAX	MAX STEP RELAX	RELAXATION CYCLE	INITIAL TIME	FINAL TIME	IMPR. STEPS
601	40	.0001	.01	8	-1.5708	1.5708	100

SPECIAL SPAN LOCATION	TIP LOCATION	GEOM. SYMMETRY Y/N	BASIC THICKNESS	ASPECT RATIO
.9	1.	1	.12	7.

ROOT SYM CONDITION Y/N	UP-LO SYMMETRY Y/N	LATERAL GRADIENT Y/N
0	1	1

NO.X MESH	NO.Y MESH	NO.Z MESH
64	32	32

LEADING EDGE	TRAILING EDGE	SPECIAL SPAN NO.	TIP NO.	LOWER SURFACE NO.	UPPER S.NO.
18	48	11	21	16	17

MIN.X SURFACE	MAX.X SURFACE	MIN.Y SURFACE	MAX.Y SURFACE	MIN.Z SURFACE	MAX.Z SURFACE
-8.0	6.0	.5	1.5849	-3.	3.

14

BASIC PROFILE

NO.POINTS	INDEX	ABSCISSA	ORDINATE
101			
	1	1.0000	.0013
	2	.9990	.0014
	3	.9961	.0018
	4	.9911	.0025
	5	.9843	.0034
	6	.9755	.0046
	7	.9649	.0061
	8	.9524	.0077
	9	.9382	.0096
	10	.9222	.0117
	11	.9045	.0139
	12	.8853	.0163
	13	.8645	.0188
	14	.8423	.0214
	15	.8187	.0241
	16	.7939	.0269
	17	.7679	.0297
	18	.7409	.0325
	19	.7129	.0354
	20	.6841	.0382
	21	.6545	.0409
	22	.6243	.0436
	23	.5937	.0461
	24	.5627	.0486
	25	.5314	.0509
	26	.5000	.0529
	27	.4686	.0548
	28	.4373	.0564
	29	.4063	.0578
	30	.3757	.0588
	31	.3455	.0596
	32	.3159	.0600
	33	.2871	.0600
	34	.2591	.0596
	35	.2321	.0589
	36	.2061	.0577
	37	.1813	.0562
	38	.1577	.0542
	39	.1355	.0519
	40	.1147	.0491
	41	.0955	.0460
	42	.0778	.0426

BASIC PROFILE
NO. POINTS INDEX ABSCISSA ORDINATE
101

INDEX	ABSCISSA	ORDINATE
43	.0618	.0389
44	.0476	.0348
45	.0351	.0305
46	.0245	.0259
47	.0157	.0211
48	.0089	.0161
49	.0039	.0109
50	.0010	.0055
51	.0000	.0000
52	.0010	-.0055
53	.0039	-.0109
54	.0089	-.0161
55	.0157	-.0211
56	.0245	-.0259
57	.0351	-.0305
58	.0476	-.0348
59	.0618	-.0389
60	.0778	-.0426
61	.0955	-.0460
62	.1147	-.0491
63	.1355	-.0519
64	.1577	-.0542
65	.1813	-.0562
66	.2061	-.0577
67	.2321	-.0589
68	.2591	-.0596
69	.2871	-.0600
70	.3159	-.0600
71	.3455	-.0596
72	.3757	-.0588
73	.4063	-.0578
74	.4373	-.0564
75	.4686	-.0548
76	.5000	-.0529
77	.5314	-.0509
78	.5627	-.0486
79	.5937	-.0461
80	.6243	-.0436
81	.6545	-.0409
82	.6841	-.0382
83	.7129	-.0354
84	.7409	-.0325
85	.7679	-.0297
86	.7939	-.0269
87	.8187	-.0241
88	.8423	-.0214

16

BASIC PROFILE

NO. POINTS	INDEX	ABSCISSA	ORDINATE
101			
	89	.8645	-.0188
	90	.8853	-.0163
	91	.9045	-.0139
	92	.9222	-.0117
	93	.9382	-.0096
	94	.9524	-.0077
	95	.9649	-.0061
	96	.9755	-.0046
	97	.9843	-.0034
	98	.9911	-.0025
	99	.9961	-.0018
	100	.9990	-.0014
	101	1.0000	-.0013

SUBROUTINE MESH

```
      DUM=(YIJ-YIC)/(YID-YIC)
      Y(J)=YC+DUM*(YD-YC)
      GO TO 4
    2 CONTINUE
      DUM=-.5*PI*(YIJ-YIC)/YIC
      DUM=COS(DUM)
      Y(J)=YN+DUM*(YC-YN)
      GO TO 4
    3 CONTINUE
      DUM=.5*PI*(YIJ-YID)/(1.-YID)
      DUM=COS(DUM)
      Y(J)=YX+DUM*(YD-YX)
    4 CONTINUE
      IF(JSYM.NE.1) Y(1)=Y(2)
      WRITE(6,1000)
      DO 5 J=1,JM
      WRITE(6,1001) J,YI(J),Y(J)
    5 CONTINUE
C*****PLANFORM EQUATION XA(J),XF(J)
      DO 6 J=1,JM
      YJ=Y(J)
      XA(J)=0.
      XF(J)=1.
      IF(J.LE.JC) GO TO 6
      XA(J)=3.531767*(YJ-YC)
      XF(J)=1.+XA(J)
      IF(J.LE.JD) GO TO 6
      XA(J)=XA(J-1)
      XF(J)=XF(J-1)
    6 CONTINUE
      XA(1)=XA(2)
      XF(1)=XF(2)
      WRITE(6,1002)
      DO 7 J=1,JM
      WRITE(6,1001) J,XA(J),XF(J)
    7 CONTINUE
      XII=-1.-DXI
      DO 8 I=1,IM
      XII=XII+DXI
      XI(I)=XII
    8 CONTINUE
      I=0
```

18

REFERENCES

1. Isom, M. P.: Unsteady Subsonic and Transonic Potential Flow Over Helicopter Rotor Blades. NASA CR-2463, 1974.

2. Murman, E. M.; and Cole, J. D.: Calculation of Plane Steady Transonic Flows. AIAA J., vol. 9, 1971, pp. 114-121.

3. Murman, E. M., Analysis of Embedded Shock Waves Calculated by Relaxation Methods. Proceedings of AIAA Computational Fluid Dynamics Conference, Palm Springs, California, July 1973, pp. 27-40.

4. Caradonna, F. X.; and Philippe, J. J.: The Flow Over a Helicopter Blade Tip in the Transonic Regime. Vertica, 1978, vol. 2, pp. 43-60.

5. Caradonna, F. X.; and Steger, J. L.: Implicit Potential Methods for the Solution of Transonic Rotor Flows. Presented at the 1980 Army Numerical Analysis and Computers Conference, Feb. 20-21, 1980, Moffett Field, California.

6. Philippe, J. J.; and Armand, C.: Rotorcraft Design. AGARD CP-233, presented at the Proceedings of the Flight Mechanics Panel Symposium, Moffett Field, Calif., May 16-19, 1977.
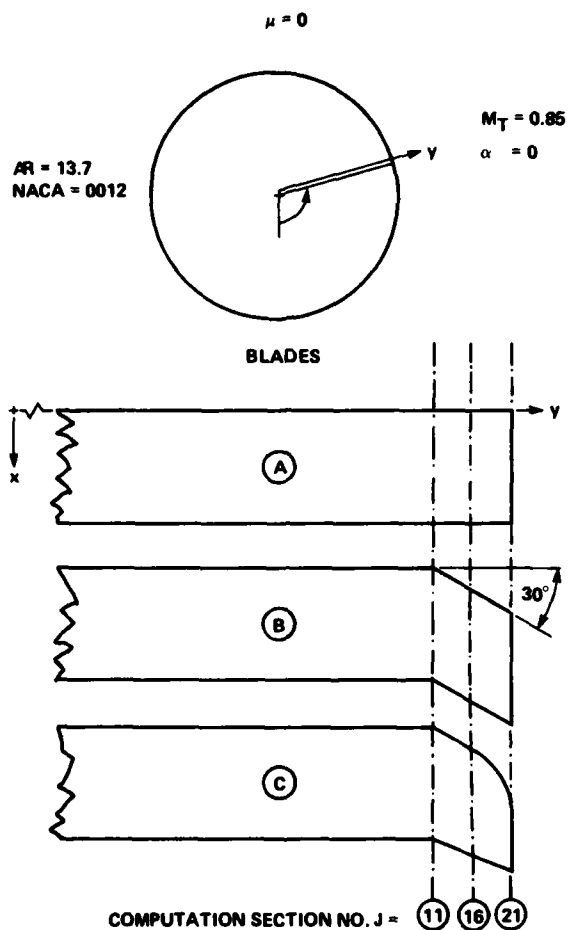
Figure 1.- Simulations of three-dimensional steady (hover) flows for: A - a rectangular blade; B - a swept-tip blade; and C - a combination of swept- and parabolic-tip blade.

20

BLADE A

$\gamma = 0.949$

(a) Station J = 11.

BLADE A

$\gamma = 0.9745$

(b) Station J = 16.

BLADE A

$\gamma = 1$

(c) Station J = 21.

BLADE B

$\gamma = 0.949$
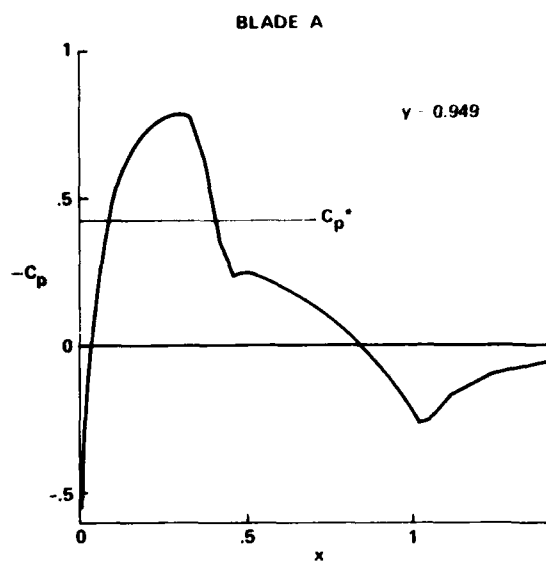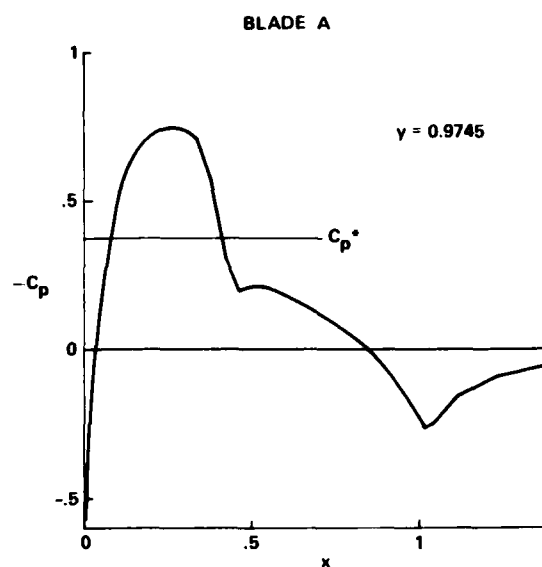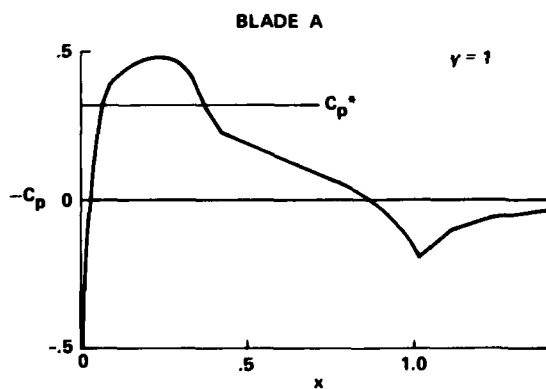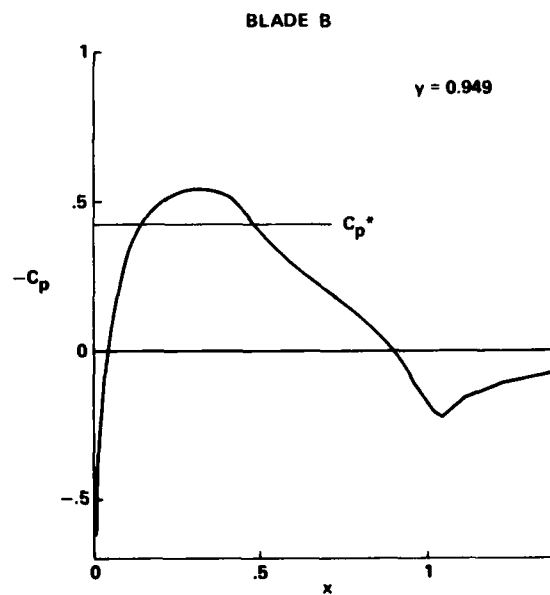
(d) Swept tip, station J = 11.

Figure 2.- Pressure distribution computations; tip in hover.
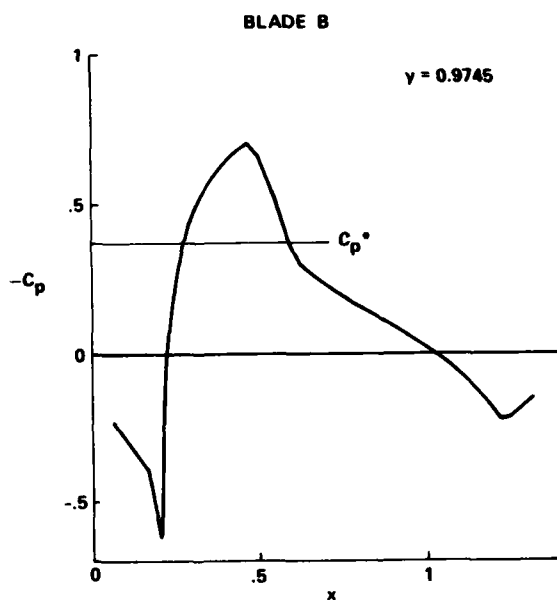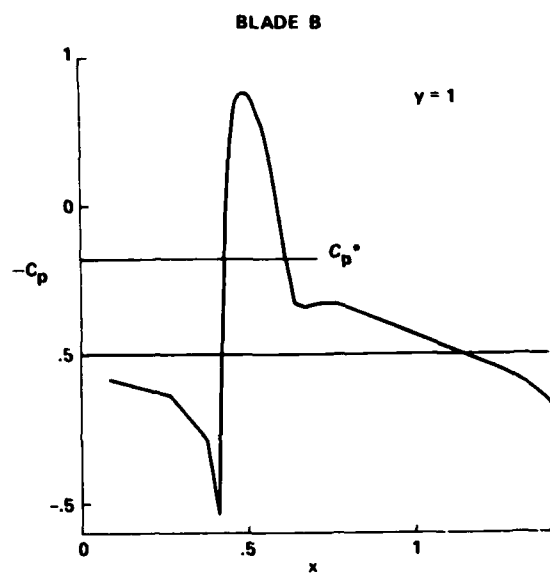
(e) Swept tip, station J = 16.   (f) Swept tip, station J = 21.

Figure 2.- Continued.

22

BLADE C

$\gamma = 0.949$

BLADE C

$\gamma = 0.9745$
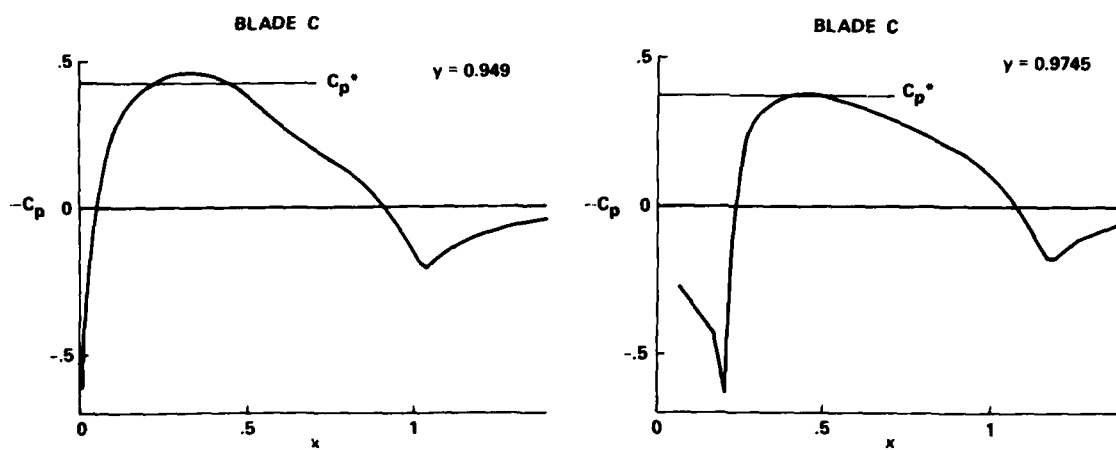
(g) Swept tip, station J = 11.   (h) Swept tip, station J = 16.

BLADE C

$\gamma = 1$
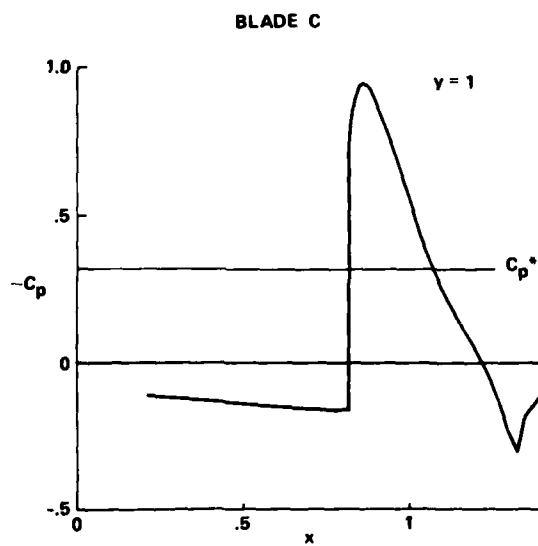
(i) Swept tip, station J = 21.

Figure 2.- Concluded.

23

$\mu = 0.45$, 0.50, and 0.55

AR = 7

M = 0.6
$\alpha = 0$

RECTANGULAR BLADE

COMPUTATION SECTION NO. ⑪ ⑯ ㉑

EXPERIMENTAL DATA SECTION NO. ② ③
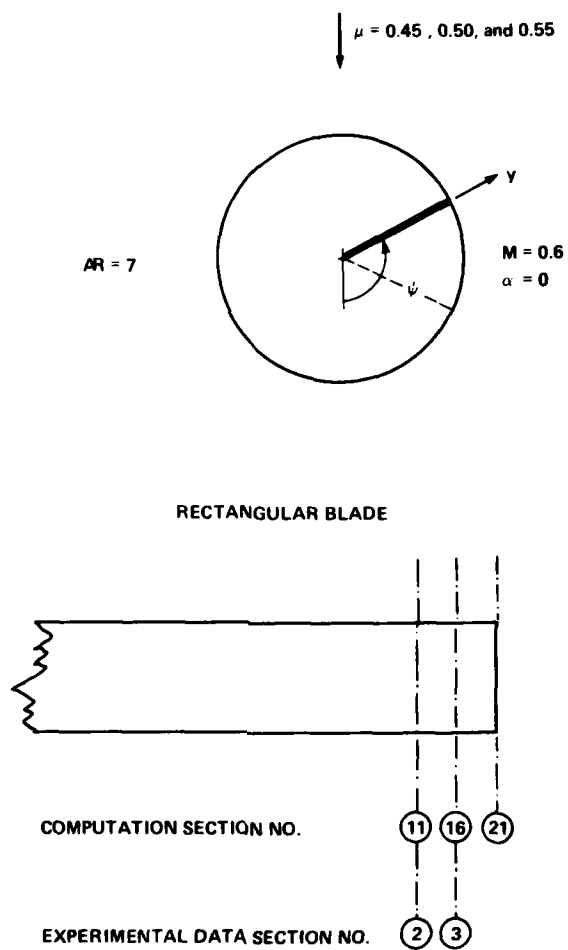
Figure 3.– Three-dimensional unsteady problem for forward flight.

○ EXPERIMENT
— THEORY

$\psi = 60°$
$\gamma = 0.9$
$\mu = 0.45$

C_p^*

1.0

.5

$-C_p$

0

-.5

0 .5 1
x

(a) Station 11.

○ EXPERIMENT
— THEORY

$\psi = 60$
$\gamma = 0.95$
$\mu = 0.45$

C_p^*

1

.5

$-C_p$

0

-.5

0 .5 1
x

(b) Station 16.

$\psi = 60°$
$\gamma = 1$
$\mu = 0.45$

C_p^*

1

.5

$-C_p$

0

-.5

0 .5 1
x

(c) Station 21.

○ EXPERIMENT
— THEORY

$\psi = 120°$
$\gamma = 0.9$
$\mu = 0.45$

C_p^*

1

.5

$-C_p$

0

-.5

0 .5 1
x
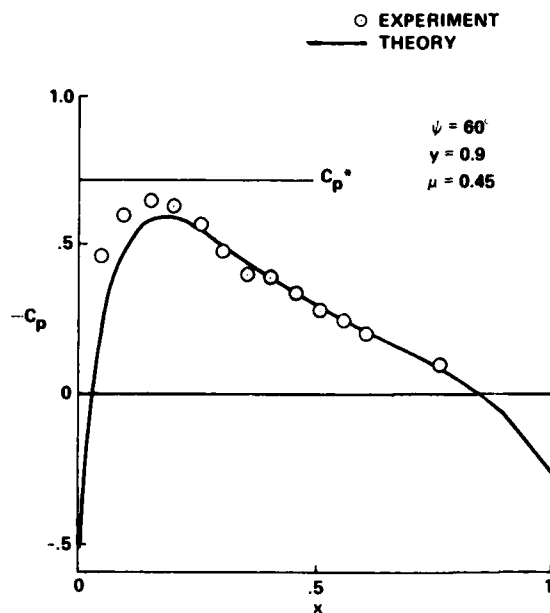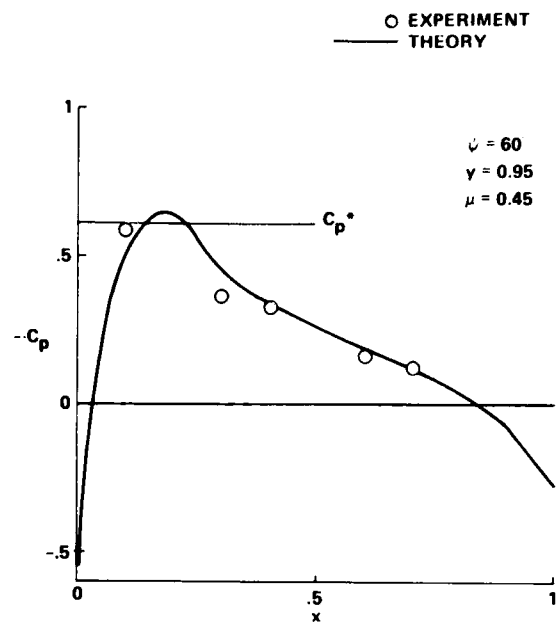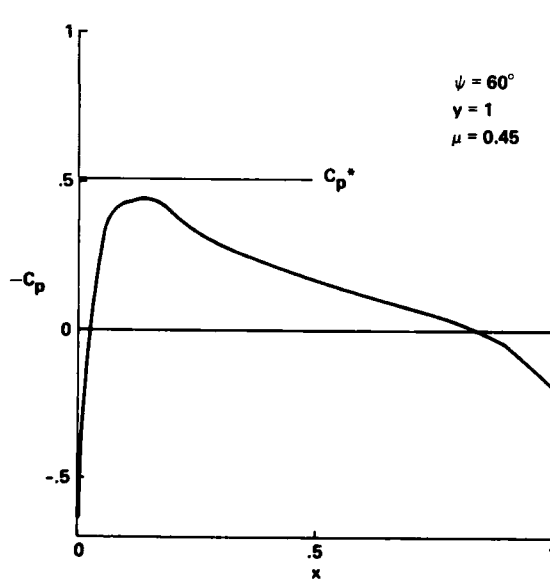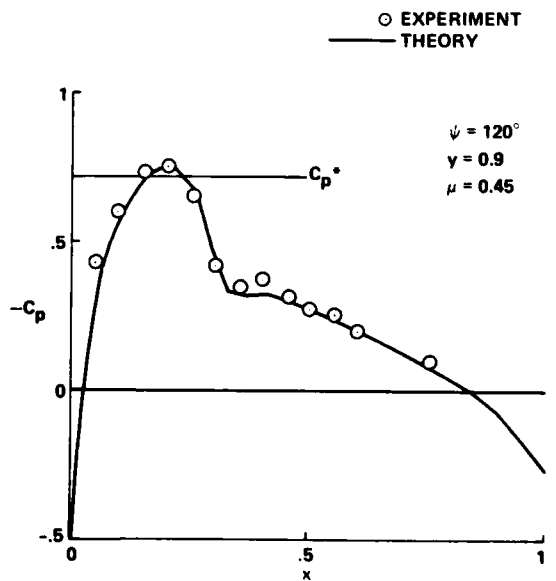
(d) Station 11.

Figure 4.- Pressure distribution computations. Symbols denote data from reference 4.
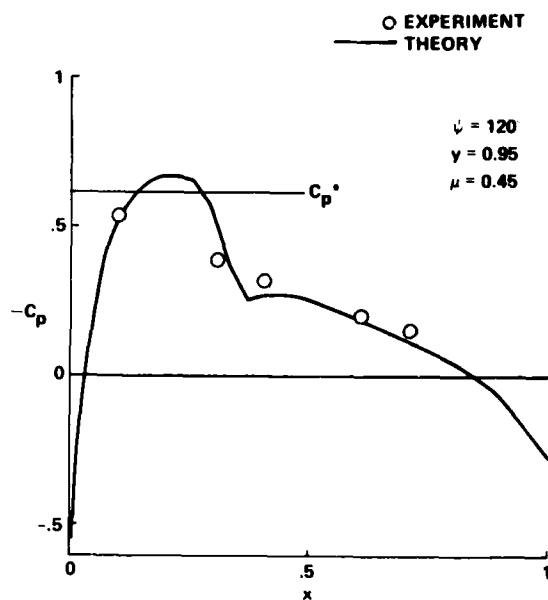
(e) Station 16.
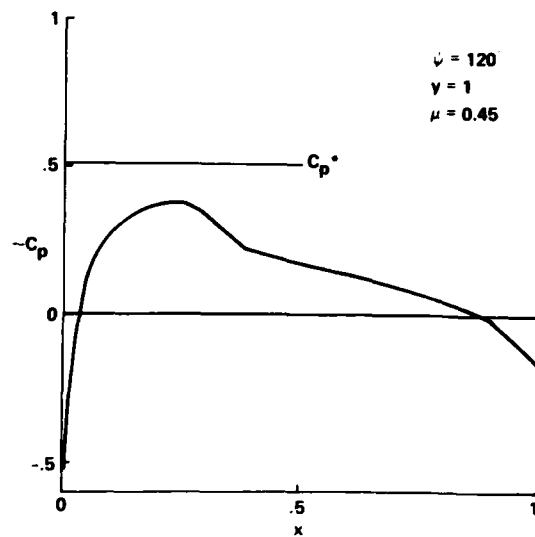
(f) Station 21.
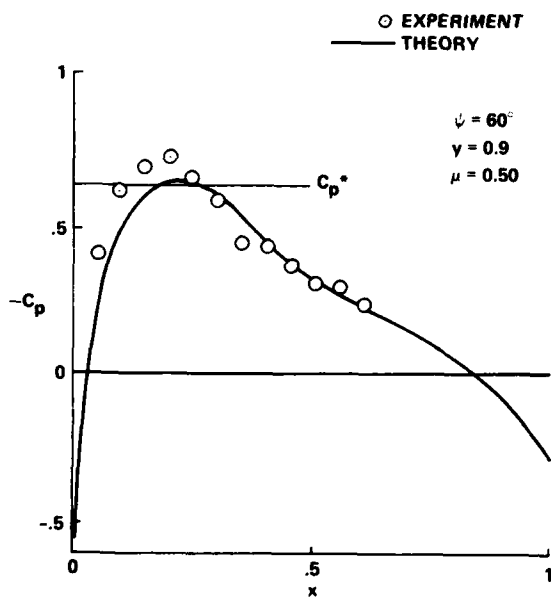
(g) Station 11.
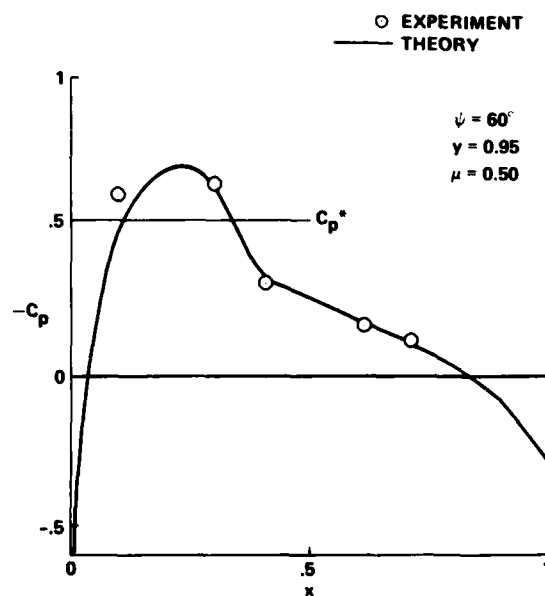
(h) Station 16.

Figure 4.- Continued.

26
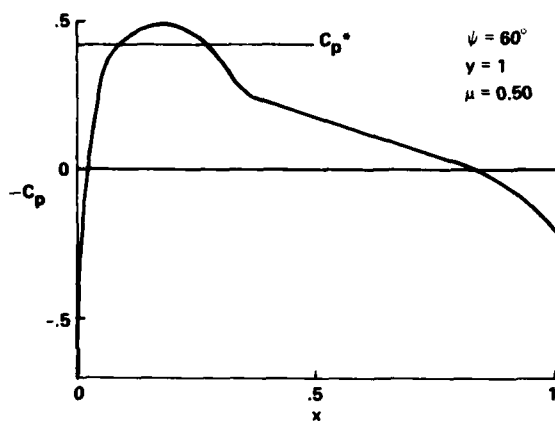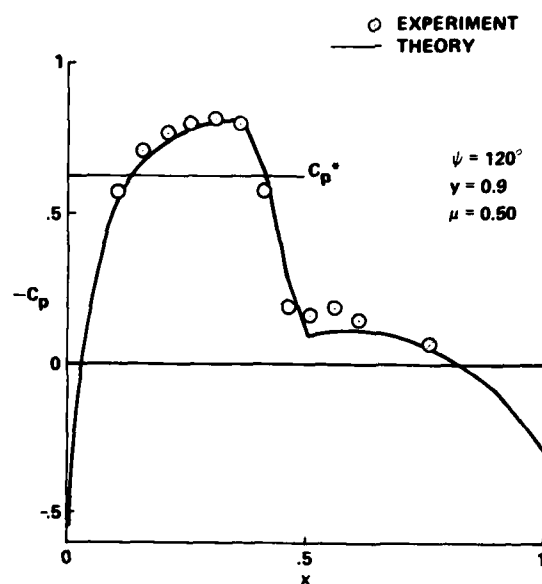
(i) Station 21.

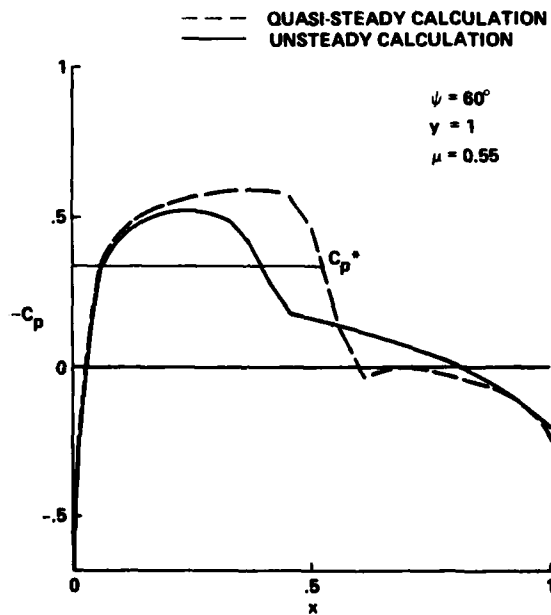(j) Station 11.
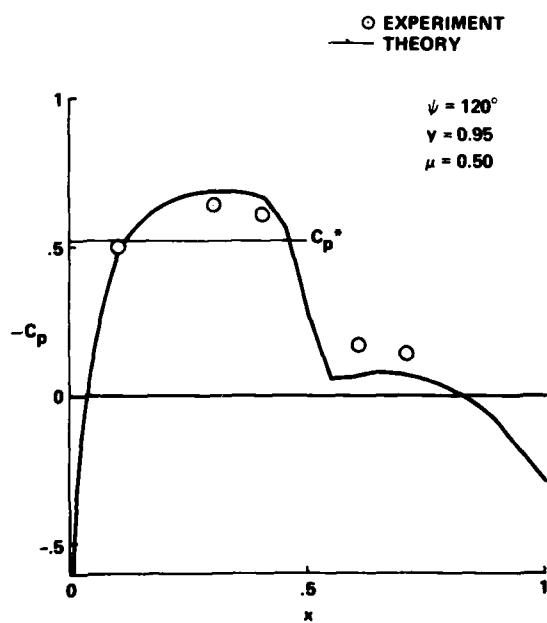
(k) Station 16.
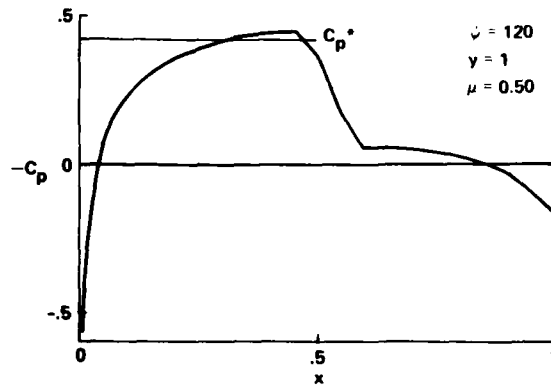
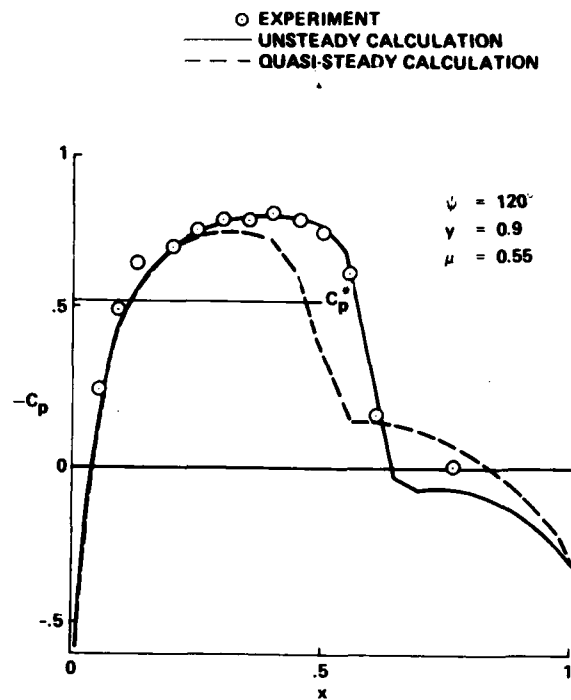(l) Station 21.

Figure 4.- Continued.
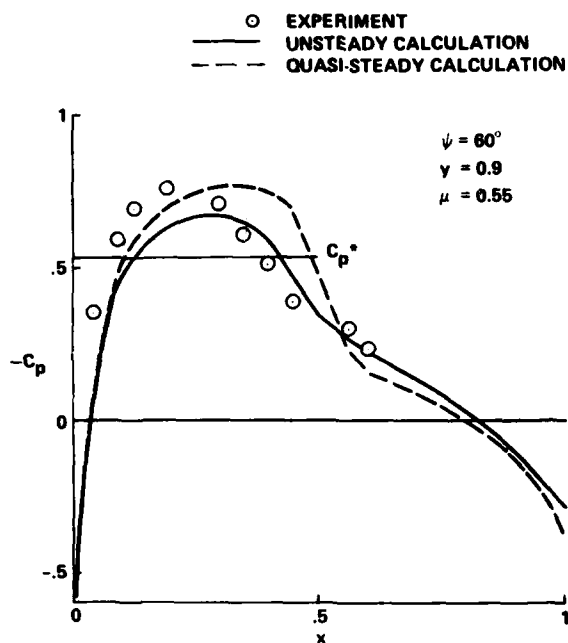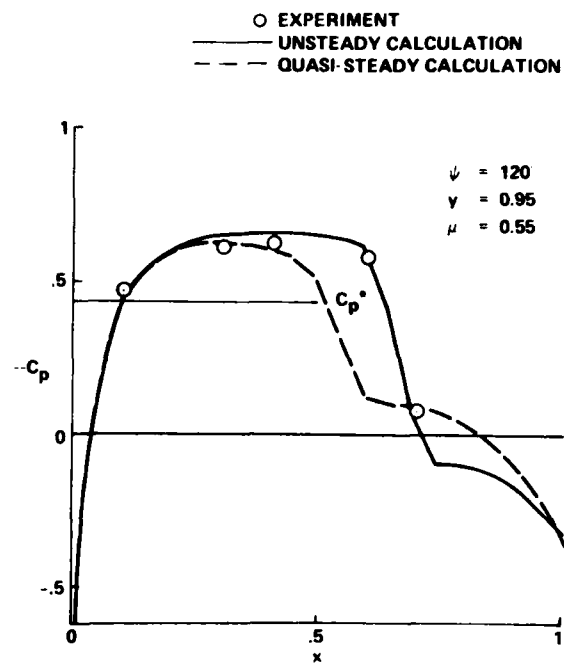
(m) Station 11.
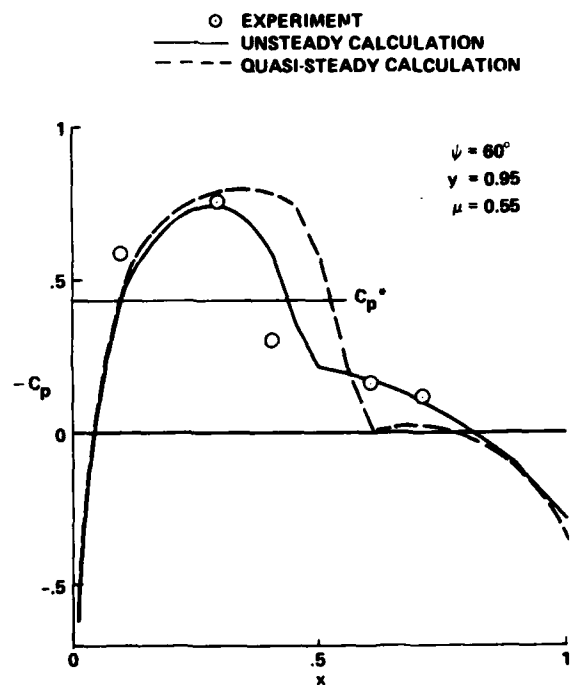
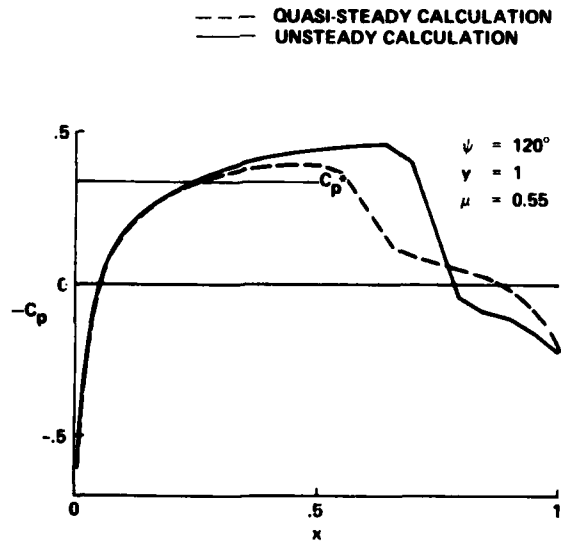(n) Station 16.

(o) Station 21.

Figure 4.- Continued.

(p) Station 11.

(q) Station 16.

(r) Station 21.

Figure 4.- Concluded.

1. Report No. NASA TP-1721 AVRADCOM TR 80-A-2	2. Government Accession No. AD-A091 1	3. Recipient's Catalog No.
4. Title and Subtitle CALCULATION OF THREE-DIMENSIONAL UNSTEADY TRANSONIC FLOWS PAST HELICOPTER BLADES*		5. Report Date October 1980
		6. Performing Organization Code
7. Author(s) J. J. Chattot		8. Performing Organization Report No. A-8024
		10. Work Unit No. 505-42-21
9. Performing Organization Name and Address NASA Ames Research Center and Aeromechanics Laboratory AVRADCOM Research and Technology Laboratories Moffett Field, CA 94035		11. Contract or Grant No.
		13. Type of Report and Period Covered Technical Paper
12. Sponsoring Agency Name and Address National Aeronautics and Space Administration Washington, DC 20546 and U.S. Army Aviation Research and Development Command St. Louis, MO 93166		14. Sponsoring Agency Code

15. Supplementary Notes
*Work done while author was an exchange scientist under the Memorandum of Understanding between the U.S. Army Aeromechanics Laboratory, AVRADCOM, and Ames Research Center, Moffett Field, Calif., and ONERA, France.

16. Abstract

A finite difference code for predicting the high-speed flow over the advancing helicopter rotor is presented. The code solves the low-frequency, transonic small disturbance equation and is suitable for modeling the effects of advancing blade unsteadiness on blades of nearly arbitrary planform. The method employs a quasi-conservative mixed differencing scheme and solves the resulting difference equations by an alternating direction scheme. Computed results show good agreement with experimental blade pressure data and illustrate some of the effects of varying the rotor planform. The flow unsteadiness is shown to be an indispensible part of a transonic solution. It is also shown that, close to the tip at high advance ratio, cross-flow effects can significantly affect the solution.

17. Key Words (Suggested by Author(s)) Aerodynamics Numerical analysis Unsteady flow, Transonic flow Helicopter aerodynamics	18. Distribution Statement Unclassified – Unlimited STAR Category 02		
19. Security Classif. (of this report) Unclassified	20. Security Classif. (of this page) Unclassified	21. No. of Pages 31	22. Price* A03

30